

Ferromagnetic Resonance Frequency Shift in Yttrium Iron Garnet

C. W. HAAS,* T. J. MATCOVICH, H. S. BELSON,† AND N. GOLDBERG
UNIVAC, Division of Sperry Rand Corporation, Blue Bell, Pennsylvania

(Received 16 July 1963)

Calculations and measurements have been made of the shift of the ferromagnetic resonance frequency in the presence of excited magnons. The calculations were carried out by retaining terms in the Hamiltonian up to fourth order in the spin-wave variables and by treating these terms in a random phase approximation. The frequency shift depends linearly on the number of excited $k=0$ and $k\neq 0$ magnons, with a k -dependent proportionality factor. Measurements of this shift therefore can be used to determine the magnon distribution at resonance, and such measurements have been used to study the effect of surface preparation of the sample on the magnon distribution. The results show considerable agreement with the surface pit model; namely, the linewidth and the number of $k\neq 0$ magnons increase with increased surface roughness, the surface-induced scattering from the $k=0$ mode occurs to a localized group of degenerate $k\neq 0$ spin waves, and the effective wavelength of the spin wave to which scattering occurs increases with increased surface roughness. The data are not consistent with the theory that there is a rapid equilibration of the degenerate spin waves. The frequency shift was also observed at power levels above the critical value for the onset of nonlinearities. The results cannot be explained simply by invoking the instability of $\theta_k=0$ spin waves. Possible alternate explanations are offered.

I. INTRODUCTION

IN general, there are a number of relaxation mechanisms which contribute to the ferromagnetic resonance linewidth. Therefore, even if the resonance linewidth is measured as a function of the various parameters (temperature, frequency, surface roughness, degree of ionic disorder, impurities, etc.), it is often difficult to determine the relative importance of the various relaxation mechanisms. Several methods have been developed which permit the relaxation processes to be studied in greater detail.¹⁻⁴ As we shall show, a useful approach to this problem is to measure the shift of the resonance frequency as a function of the rf power absorbed by the sample.^{5,6}

In a typical low-power ferromagnetic resonance experiment, the rf field excites a steady supply of $k=0$ magnons. These magnons can relax to the lattice either by relaxing first to other magnons and then to the lattice, or by relaxing directly to the lattice. Therefore, there is a magnon population composed of $k=0$ and $k\neq 0$ magnons in excess of the thermal number. As the amount of power absorbed by the sample increases, the number of $k=0$ magnons (n_0) and the number of $k\neq 0$ magnons (n') also increases. It will be shown that there is a shift in the resonance frequency with increasing absorbed power, and the shift can be expressed as a function of n_0 and n' . Measurement of this shift, therefore, provides information concerning the equilibrium

magnon population at resonance. Direct information concerning this magnon population has not heretofore been available, and such information can be very useful in determining the relative importance of the various relaxation mechanisms.

In the usual derivation of the $k=0$ spin-wave resonance frequency, terms in the Hamiltonian higher than second order in the spin-wave annihilation and creation operators are ignored. The higher order terms represent interactions among the spin waves. If these terms are retained, the resonance frequency is shifted, and the magnitude of the shift depends on the degree of excitation of the various spin waves.

Physically one can imagine several sources for a resonance frequency shift:

(1) The excitation of magnons (both $k=0$ and $k\neq 0$) results in a decrease in M_z . In a nonspherical sample, this decrease in M_z changes the macroscopic demagnetizing fields, and therefore, also changes the resonance frequency.

(2) The excitation of $k\neq 0$ magnons results in local demagnetizing fields which also affect the resonance frequency. This effect is important in spherical, as well as in nonspherical, samples.

(3) As the rf power increases, the excitation of $k=0$ magnons causes the angle of the precessional cone of the magnetization to increase. This changes the effective field due to the magnetocrystalline anisotropy energy since the effective field depends on the crystallographic direction of the magnetization, and thereby the resonance frequency is changed.

(4) Although the presence of $k\neq 0$ magnons does not cause tilting of the average magnetization, the individual spins are tilted. Thus, the effective field due to the magnetocrystalline anisotropy energy is also changed by $k\neq 0$ excitations.

Since we are interested in gaining information about relaxation processes, we do not include in our considera-

* Present address: Central Research Department, E. I. Dupont de Nemours & Company, Wilmington, Delaware.

† Present address: Naval Ordnance Laboratory, White Oak, Silver Spring, Maryland.

¹ H. Suhl, *J. Phys. Chem. Solids* **1**, 209 (1957).

² E. Schlömann, J. J. Green, and U. Milano, *J. Appl. Phys.* **31**, 386S (1960).

³ C. Kittel, *Phys. Rev.* **110**, 1295 (1958).

⁴ R. C. Fletcher, R. C. LeCraw, and E. G. Spencer, *Phys. Rev.* **117**, 955 (1960).

⁵ T. J. Matcovich, H. S. Belson, and N. Goldberg, *J. Appl. Phys.* **32**, 163S (1961).

⁶ T. J. Matcovich, H. S. Belson, N. Goldberg, and C. W. Haas, *J. Appl. Phys.* **33**, 1287 (1962).

tions the thermal shift, i.e., the shift of the resonance frequency due to the thermal excitation of magnons. Thus, the number of magnons which we find are the excess over the thermal number.

It is well known that the resonance frequency of any system is shifted if there are losses present. In yttrium iron garnet, this direct effect of the losses is quite small, and indeed it is negligible compared to the shift we calculate and measure. Of course, the $k \neq 0$ portion of the frequency shift with which we are concerned is dependent upon the presence of loss mechanisms, for in the absence of loss, n' would be zero. However, we are concerned with the effect of the population of these magnons on the resonance frequency rather than the effect of the spin-wave scattering which produces them.

In Sec. II, we outline the derivation of the expression for the shift in the resonance frequency as a function of n_0 and n' . The frequency shift is found to be proportional to n_0 and n' . While we give a spin-wave derivation, similar results can be obtained from a Green function calculation.⁷ Section III contains a description of the experimental procedure. The experimental results and conclusions connected with a study of the effect of sample surface preparation on the magnon distribution in yttrium iron garnet is the topic of Sec. IV. This study was done by observing the resonance frequency shift and the linewidth of a sphere of yttrium iron garnet as a function of surface roughness. The data show considerable agreement with the predictions of the pit-scattering theory of Sparks, Loudon, and Kittel⁸: the linewidth and n' increase with increased surface roughness; the surface induced scattering from the $k=0$ mode occurs to a localized group of degenerate $k \neq 0$ spin waves; the effective wavelength of the spin wave to which scattering occurs increases with increased surface roughness. However, the data are not consistent with a rapid equilibration of the degenerate or S spin waves as predicted by Sparks, Loudon, and Kittel.⁸

The shift in the resonance frequency is not directly associated with the nonlinear instabilities,^{1,2} and all the observations discussed in Sec. IV were made with the rf intensity below the critical value for the onset of nonlinearities. However, the frequency shift has also been studied as the rf intensity is increased above the critical value, and these results, together with the predictions based on the usual second-order Suhl theory,^{9,10} are discussed in Sec. V. The frequency shift results cannot be explained simply by invoking the instability of $\theta_k=0$ spin waves. Possible alternative explanations are offered.

⁷ C. W. Haas, Phys. Rev. **132**, 228 (1963).

⁸ M. Sparks, R. Loudon, and C. Kittel, Phys. Rev. **122**, 791 (1961).

⁹ H. Suhl, J. Phys. Chem. Solids **1**, 209 (1957).

¹⁰ E. Schlömann, Tech. Report R-48 Research Division, Raytheon Company, Waltham, Massachusetts, 1959 (unpublished).

II. DERIVATION OF THE FREQUENCY SHIFT EXPRESSION

We consider the Hamiltonian which is composed of the Zeeman energy, the nearest-neighbor exchange energy, the magnetic dipolar energy, and the magneto-crystalline anisotropy energy. Schlömann^{10,11} has treated such a Hamiltonian in connection with his studies of high power effects. He uses a semiclassical formulation by which he obtains the equations of motion of the spin-wave amplitudes from his spin-wave Hamiltonian. As part of his studies of high-power effects, Schlömann finds the shift in the resonance frequency of the uniform mode which arises from the excitation of $k=0$ and z directed $k \neq 0$ spin waves. The excitation of these spin waves result in an increase in the resonance frequency. In general, however, the excitation of spin waves can result in either an increase or a decrease in the resonance frequency depending upon the particular spin waves being excited and upon the crystallographic direction along which the magnetization vector lies.

In a calculation independent of ours, Oguchi and Honma¹² calculated the effect of the excitation of $k \neq 0$ magnons on the resonance frequency of the uniform mode in order to corroborate the correct temperature dependence of the resonance frequency. They consider the effects of the dipolar interaction and the magneto-crystalline anisotropy energy separately while we treat both terms simultaneously. The only difference in the results is a modification of the anisotropy contribution in our expression for the frequency shift. This modification arises from the Holstein-Primakoff transformation¹³ which diagonalizes the second-order terms in the complete Hamiltonian. However, contrary to the suggestion of Oguchi and Honma, the effect of the dipolar interaction on the resonance frequency may not be neglected in the case of spherical samples. This can be concluded from both our results and theirs. In fact, the effect of the dipolar interaction on the resonance frequency of a spherical sample plays a very important role in the extraction of information from the measured frequency shift.

We have used Schlömann's formulation in what follows. While Oguchi and Honma carry out a quantum mechanical calculation, the results of the two treatments are identical.

Following Schlömann, we let $\alpha(\mathbf{r})$ be the unit vector pointing in the direction of the magnetization at point \mathbf{r} :

$$\alpha(\mathbf{r}) = \mathbf{M}_0(\mathbf{r})/M_0, \quad (1)$$

where M_0 is the saturation magnetization at the ambient temperature.

The equations of motion are usually expressed in terms of the Fourier components of $\alpha_x(\mathbf{r})$ and $\alpha_y(\mathbf{r})$. The variables $\alpha_x(\mathbf{r})$ and $\alpha_y(\mathbf{r})$ behave as conjugate coordi-

¹¹ E. Schlömann, Phys. Rev. **116**, 828 (1959).

¹² T. Oguchi and A. Honma, J. Phys. Soc. Japan **16**, 79 (1961).

¹³ T. Holstein and H. Primakoff, Phys. Rev. **58**, 1098 (1940).

nates and momenta in the limits of small amplitude. Schlömann introduces variables $s(\mathbf{r})$ and $s^*(\mathbf{r})$ in terms of which the equations of motion have canonical form for arbitrary amplitudes. The new variables are related to the old by the transformation

$$\alpha_x = \frac{1}{2}(s + s^*)[1 - \frac{1}{4}(s^*s)]^{1/2}, \quad (2)$$

$$\alpha_y = (s - s^*)[1 - \frac{1}{4}(s^*s)]^{1/2}/2i, \quad (3)$$

$$\alpha_z = 1 - \frac{1}{2}(s^*s). \quad (4)$$

The variables $s(\mathbf{r})$ can be expressed in terms of the Fourier components $s_{\mathbf{k}}$

$$s(\mathbf{r}) = \sum_{\mathbf{k}} s_{\mathbf{k}} e^{i\mathbf{k}\cdot\mathbf{r}}. \quad (5)$$

The equations of motion are

$$s_{\mathbf{k}} = i \frac{\partial \mathcal{C}}{\partial s_{\mathbf{k}}^*}, \quad (6)$$

where

$$\mathcal{C} = \frac{2\gamma}{VM_0} \int E d^3r \quad (7)$$

and E is the energy density. The integration extends over the periodicity volume V .

The energy density will include four parts: the Zeeman energy, the exchange energy, the dipolar energy, and the magnetocrystalline anisotropy energy. We restrict ourselves to the case of a sample which exhibits cubic symmetry. Furthermore, in this paper, we consider a sample which is an ellipsoid of revolution with the axis of revolution being coincident with either the [100] or [111] crystallographic direction.¹⁴ We choose the dc magnetic field along the axis of revolution so that the equilibrium direction of the magnetization is coincident with the axis of revolution.

Schlömann¹⁰ has shown in detail how the contribution to the Hamiltonian of each term in E can be expressed in terms of the spin-wave amplitudes $s_{\mathbf{k}}$ and $s_{\mathbf{k}}^*$. We first consider that part of the contribution of the anisotropy energy to the Hamiltonian which affects the resonance frequency of the uniform mode. Using Schlömann's expressions we find

$$\mathcal{C}_{\text{anis}} = 2\gamma \frac{K_{10}}{M_0} \alpha^{[i]} s_0^* s_0 [1 - \frac{9}{2} \sum_{\mathbf{k} \neq 0} s_{\mathbf{k}}^* s_{\mathbf{k}} - (9/8) s_0^* s_0], \quad (8)$$

where K_{10} is the first-order anisotropy coefficient at the ambient temperature, and

$\alpha^{[i]} = 1$ if $[i]$ denotes the [100] crystallographic direction, $\alpha^{[i]} = -\frac{2}{3}$ if $[i]$ denotes the [111] crystallographic direction.

¹⁴ The case of the [110] crystallographic direction coincident with the axis of revolution has also been treated. See C. W. Haas, Ph.D. thesis, University of Pennsylvania, Philadelphia, Pennsylvania (unpublished).

The excitation of $k=0$ magnons alters the anisotropy contribution to the Hamiltonian by the factor

$$[1 - (9/8) s_0^* s_0]. \quad (9)$$

The form of this factor is dictated by the angular dependence of the cubic anisotropy energy which of course has been well confirmed experimentally.

The excitation of $k \neq 0$ magnons alters the anisotropy contribution to the Hamiltonian by the factor

$$1 - \frac{9}{2} \sum_{\mathbf{k} \neq 0} s_{\mathbf{k}}^* s_{\mathbf{k}}. \quad (10)$$

The origin of this factor can be seen as follows: The thermal excitation of magnons results in the temperature dependence of the anisotropy constant K_1 . From very general theoretical arguments, it can be shown¹⁵ that the temperature dependence of K_1 can be represented by the 10th power law, i.e.,

$$K_1 = K_{10} (1 - 10(M - M_0)/M_0) \\ = K_{10} \left(1 - \frac{10\gamma\hbar}{M_0} \sum_{\mathbf{k} \neq 0} n_{\mathbf{k}} \right), \quad (11)$$

where

$$n_{\mathbf{k}} = M_0 s_{\mathbf{k}}^* s_{\mathbf{k}} / 2\gamma\hbar \quad (12)$$

is the number of $k \neq 0$ magnons. Also,

$$M = M_0 \left(1 - \frac{\gamma\hbar}{M_0} \sum_{\mathbf{k} \neq 0} n_{\mathbf{k}} \right). \quad (13)$$

Therefore,

$$\frac{K_1}{M} \approx \frac{K_{10}}{M_0} \left(1 - \frac{9}{2} \sum_{\mathbf{k} \neq 0} s_{\mathbf{k}}^* s_{\mathbf{k}} \right). \quad (14)$$

However, the theoretical predictions do not agree with observation.¹⁶ Rather than introduce this erroneous theoretical dependence into the frequency shift expression, we prefer to introduce the empirical dependence. That is, instead of using Eq. (14), we write Eq. (11) as

$$K_1 = K_{10} \left(1 - \frac{C\gamma\hbar}{M_0} \sum_{\mathbf{k} \neq 0} n_{\mathbf{k}} \right), \quad (15)$$

where C is a constant to be determined experimentally, and

$$\frac{K_1}{M} = \frac{K_{10}}{M_0} \left(1 - \frac{C-1}{2} \sum_{\mathbf{k} \neq 0} s_{\mathbf{k}}^* s_{\mathbf{k}} \right). \quad (16)$$

Therefore, as the anisotropy contribution to the energy we take

$$\mathcal{C}_{\text{anis}} = \frac{2\gamma K_{10}}{M_0} \alpha^{[i]} s_0^* s_0 \\ \times \left(1 - \frac{C-1}{2} \sum_{\mathbf{k} \neq 0} s_{\mathbf{k}}^* s_{\mathbf{k}} - (9/8) s_0^* s_0 \right). \quad (17)$$

¹⁵ See, e.g., the general arguments by J. H. Van Vleck, J. Phys. Radium **20**, 124 (1959).

¹⁶ J. F. Dillon, Jr., Phys. Rev. **105**, 760 (1957).

Thus, the part of the Hamiltonian which determines the frequency of the $k=0$ mode is

$$\begin{aligned} &\gamma[H_0 - 4\pi M_0(N_z - N_t) + 2(K_{10}/M_0)\alpha^{[i]}]s_0^*s_0 + \frac{1}{4}\gamma[4\pi M_0(N_z - N_t) - 9\alpha^{[i]}(K_{10}/M_0)]s_0^{*2}s_0^2 \\ &+ \frac{1}{2}\gamma \sum_{\mathbf{k} \neq 0} \{ [4\pi M_0(N_z - N_t + 1 - \frac{3}{2}\sin^2\theta) - 2(C-1)(K_{10}/M_0)\alpha^{[i]}]s_{\mathbf{k}}^*s_{\mathbf{k}}s_0^*s_0 \\ &- \frac{1}{4}(4\pi M_0)\sin^2\theta_{\mathbf{k}}(e^{-2i\varphi_{\mathbf{k}}}s_{\mathbf{k}}s_{-\mathbf{k}} + e^{2i\varphi_{\mathbf{k}}}s_{\mathbf{k}}^*s_{-\mathbf{k}}^*)s_0^*s_0 \}. \end{aligned} \quad (18)$$

The variables s_0^* and s_0 are normal coordinates even when the dipolar interaction is included; this is not true for the variables $s_{\mathbf{k}}^*$ and $s_{\mathbf{k}}$. The normal coordinates $u_{\mathbf{k}}$ are obtained in the usual way by making the Holstein-Primakoff transformation¹³ of the form

$$s_{\mathbf{k}} = \cosh\frac{1}{2}\psi_{\mathbf{k}}\mu_{\mathbf{k}} - \sinh\frac{1}{2}\psi_{\mathbf{k}}e^{2i\varphi_{\mathbf{k}}}\mu_{-\mathbf{k}}^*, \quad (19)$$

$$s_{\mathbf{k}}^* = -\sinh\frac{1}{2}\psi_{\mathbf{k}}e^{-2i\varphi_{\mathbf{k}}}\mu_{-\mathbf{k}} + \cosh\frac{1}{2}\psi_{\mathbf{k}}\mu_{\mathbf{k}}^*, \quad (20)$$

where

$$\cosh\psi_{\mathbf{k}} = \frac{A_{\mathbf{k}}}{\omega_{\mathbf{k}}} = \frac{\gamma[H_0 - 4\pi M_0N_z + (2K_{10}/M_0)\alpha^{[i]} + H_e a^2 k^2 + 2\pi M_0 \sin^2\theta_{\mathbf{k}}]}{\omega_{\mathbf{k}}}, \quad (21)$$

$$\sinh\psi_{\mathbf{k}} = \frac{B_{\mathbf{k}}}{\omega_{\mathbf{k}}} = \frac{2\pi M_0 \gamma \sin^2\theta_{\mathbf{k}}}{\omega_{\mathbf{k}}} \quad (22)$$

and

$$\begin{aligned} \omega_{\mathbf{k}} = [A_{\mathbf{k}}^2 - B_{\mathbf{k}}^2]^{1/2} = &[(H_0 - 4\pi M_0N_z + (2K_{10}\alpha^{[i]})/M_0 + H_e a^2 k^2 + 4\pi M_0 \sin^2\theta_{\mathbf{k}}) \\ &\times (H_0 - 4\pi M_0N_z + (2K_{10}\alpha^{[i]})/M_0 + H_e a^2 k^2)]^{1/2}. \end{aligned} \quad (23)$$

Then the expression of Eq. (18), which determines the frequency of the uniform mode, can be written as

$$\begin{aligned} &\omega_0\mu_0^*\mu_0 + \frac{1}{4}\gamma \left[4\pi M_0(N_z - N_t) - 9\alpha^{[i]} \frac{K_{10}}{M_0} \right] \mu_0^{*2}\mu_0^2 \\ &+ \frac{1}{2}\gamma \sum_{\mathbf{k} \neq 0} \left\{ \left[(N_z - N_t + 1 - \frac{3}{2}\sin^2\theta_{\mathbf{k}}) \frac{(H_0 + (2K_{10}\alpha^{[i]})/M_0 - 4\pi M_0N_z + H_e a^2 k^2 + 2\pi M_0 \sin^2\theta_{\mathbf{k}})}{\omega_{\mathbf{k}}} + \frac{4\pi M_0 \sin^2\theta_{\mathbf{k}}}{4\omega_{\mathbf{k}}} \right] 4\pi M_0 \right. \\ &\left. - \frac{2(C-1)K_{10}\alpha^{[i]}}{M_0} \left(\frac{H_0 + (2K_{10}\alpha^{[i]})/M_0 - 4\pi M_0N_z + H_e a^2 k^2 + 2\pi M_0 \sin^2\theta_{\mathbf{k}}}{\omega_{\mathbf{k}}} \right) \mu_0^*\mu_{\mathbf{k}}\mu_{\mathbf{k}}^* \right\}, \end{aligned} \quad (24)$$

where

$$\omega_0 = \gamma \left[H_0 + 4\pi M_0(N_z - N_t) + 2\alpha^{[i]} \frac{K_{10}}{M_0} \right]. \quad (25)$$

The resonance frequency can be calculated directly from the equation of motion. Since the spin-wave amplitudes $u_{\mathbf{k}}$ are related to the number of magnons $n_{\mathbf{k}}$ by the expression

$$\mu_{\mathbf{k}}^*\mu_{\mathbf{k}} = 2\gamma\hbar n_{\mathbf{k}}/M_0, \quad (26)$$

the shift in the resonance frequency due to the excitation of spin waves for an ellipsoid of revolution with the dc magnetic field along the symmetry axis can be written in the form

$$\Delta f^{[i]} = a^{[i]}n_0^{[i]} + \sum_{\mathbf{k} \neq 0} b_{\mathbf{k}}^{[i]}n_{\mathbf{k}}^{[i]}, \quad (27)$$

where

$$a^{[i]} = \frac{\gamma^2\hbar}{2\pi M_0} \left[4\pi M_0(N_z - N_t) - 9\alpha^{[i]} \frac{K_{10}}{M_0} \right] \quad (28)$$

and

$$\begin{aligned} b_{\mathbf{k}}^{[i]} = \frac{\gamma^3\hbar}{2\pi M_0} \left\{ \left[4\pi M_0(N_z - N_t + 1 - \frac{3}{2}\sin^2\theta_{\mathbf{k}}) - 2\alpha^{[i]}(C-1) \frac{K_{10}}{M_0} \right] \right. \\ \left. \times \left[\frac{H_0 - 4\pi M_0N_z + 2\pi M_0 \sin^2\theta_{\mathbf{k}} + 2\alpha^{[i]}(K_{10}/M_0) + H_e a^2 k^2}{\omega_{\mathbf{k}}} + \frac{(2\pi M_0 \sin^2\theta_{\mathbf{k}})^2}{\omega_{\mathbf{k}}} \right] \right\}, \end{aligned} \quad (29)$$

where $\alpha^{[i]} = 1$ for the dc field in the [100] direction and $\alpha^{[i]} = -\frac{2}{3}$ for the dc field in the [111] direction.

The expressions for $a^{[i]}$ and $b_k^{[i]}$ simplify somewhat for the case of a spherical sample, i.e., $N_x = N_t = \frac{1}{3}$. For this case

$$a^{[i]} = (-\gamma^2 \hbar / 2\pi M_0) 9\alpha^{[i]} (K_{10}/M_0), \quad (30)$$

$$b_k^{[i]} = \frac{\gamma^3 \hbar}{2\pi M_0} \left\{ \left[4\pi M_0 (1 - \frac{3}{2} \sin^2 \theta_k) - 2\alpha^{[i]} (C-1) \frac{K_{10}}{M_0} \right] \times \frac{[H_0 + (2K_{10}\alpha^{[i]})/M_0 + H_e a^2 k^2 - (4\pi M_0/3)(1 - \frac{3}{2} \sin^2 \theta_k)]}{\omega_k} + \frac{(2\pi M_0 \sin^2 \theta_k)^2}{\omega_k} \right\}. \quad (31)$$

The value of C is required in order to calculate the b_k . It is determined as follows: Using Eqs. (12) and (13), we can rewrite Eq. (16) in the form

$$\frac{K_1}{M} = \frac{K_{10}}{M_0} \left[1 - \frac{(C-1)\gamma \hbar}{M_0} \sum_{\mathbf{k} \neq 0} n_{\mathbf{k}} \right], \quad (32)$$

$$= \frac{K_{10}}{M_0} \frac{K_{10}}{M_0} (C-1) \frac{\Delta M}{M_0}, \quad (33)$$

and see that

$$\frac{K_{10}}{M_0} \frac{(C-1)}{M_0} = \frac{d(K_1/M)}{dM}. \quad (34)$$

Thus, C can be determined experimentally from

$$\frac{K_{10}}{M_0} \frac{(C-1)}{M_0} = \frac{(d/dT)(K_1/M)}{dM/dT} \quad (35)$$

by measuring both the anisotropy constant and the magnetization and the temperature dependence of these quantities.

The value of n_0 is determined in the following manner: The rate at which $k=0$ magnons are created is $P_{\text{abs}}/V\hbar\omega_0$ where P_{abs} is the power absorbed by the sample and V is the sample volume. The rate at which $k=0$ magnons are destroyed is $\gamma\Delta H n_0$ where ΔH is the resonance linewidth. Thus, the kinetic equation for n_0 is

$$\dot{n}_0 = (P_{\text{abs}}/V\hbar\omega_0) - \gamma\Delta H n_0. \quad (36)$$

Therefore, in equilibrium

$$n_0 = P_{\text{abs}}/\gamma\hbar V\omega_0\Delta H. \quad (37)$$

It is convenient to rewrite Eq. (27) in the form

$$\frac{\Delta f^{[i]}}{n_0^{[i]}} - a^{[i]} = \frac{n'^{[i]}}{n_0^{[i]}} \sum_{\mathbf{k} \neq 0} \alpha_{\mathbf{k}}^{[i]} b_{\mathbf{k}}^{[i]}, \quad (38)$$

where $n'^{[i]}$, the total number of $k \neq 0$ magnons, and $\alpha_{\mathbf{k}}^{[i]}$, the fraction of $n'^{[i]}$ with wave vector \mathbf{k} , remain to be determined.

Even if frequency shift measurements are made on a spherical sample in two directions, [100] and [111], assumptions concerning the relaxation mechanisms based

on the properties of the sample material, surface roughness, degree of impurity, etc., will be needed in order to proceed further with the analysis. For example, consider the case in which the $k=0$ magnons relax to degenerate or S magnons which, in turn, relax rapidly either directly to the lattice, or first to other S magnons and then to the lattice. Then $\alpha_{\mathbf{k}}^{[i]}$ will be zero for all magnons except the S magnons. Further, if the scattering is independent of \mathbf{k} , $\alpha_{\mathbf{k}}$ will be a constant. Alternatively, if the scattering is strongly \mathbf{k} dependent, as for surface pit scattering, $\alpha_{\mathbf{k}}$ will be peaked about a particular \mathbf{k} . This is the case of interest to us, and we consider it further in the discussion of the results.

Finally, we consider the direct effect of the scattering mechanisms on the ferromagnetic resonance frequency. It is well known that the resonance frequency of any system is shifted if there are losses present. It is easily shown¹⁷ that the resonance frequency in the presence of losses is

$$\omega^2 = (\gamma H_0)^2 + (\frac{1}{2}\gamma\Delta H)^2. \quad (39)$$

If $\Delta H \ll H_0$, the shift in the resonance frequency due to the presence of losses is

$$\Delta f = \frac{1}{2}(\Delta H/H_0)^2 f_0, \quad (40)$$

where

$$f_0 = \gamma H_0 / 2\pi. \quad (41)$$

Since, for a typical resonance experiment on a pure YIG sample, $f_0 \approx 10^{10}$ cps and $\Delta H \approx 1$ Oe.

$$\Delta f \approx 100 \text{ cps}. \quad (42)$$

This frequency shift is very much less than those we measure which are typically of the order of 10^5 cps. In addition, the shift due to the direct effect of the scattering mechanisms should be independent of power to first order. The shift that we observe depends linearly on the power absorbed.

III. EXPERIMENTAL PROCEDURE

The resonance frequency shifts that were observed in this experiment ranged from a few tens to a few hundreds of kc/sec. In order to reliably detect such a small shift, it was necessary to reduce the errors from a number of sources. Spurious frequency shifts caused by changes in

¹⁷ See, e.g., R. W. Damon, Rev. Mod. Phys. 25, 239 (1953).

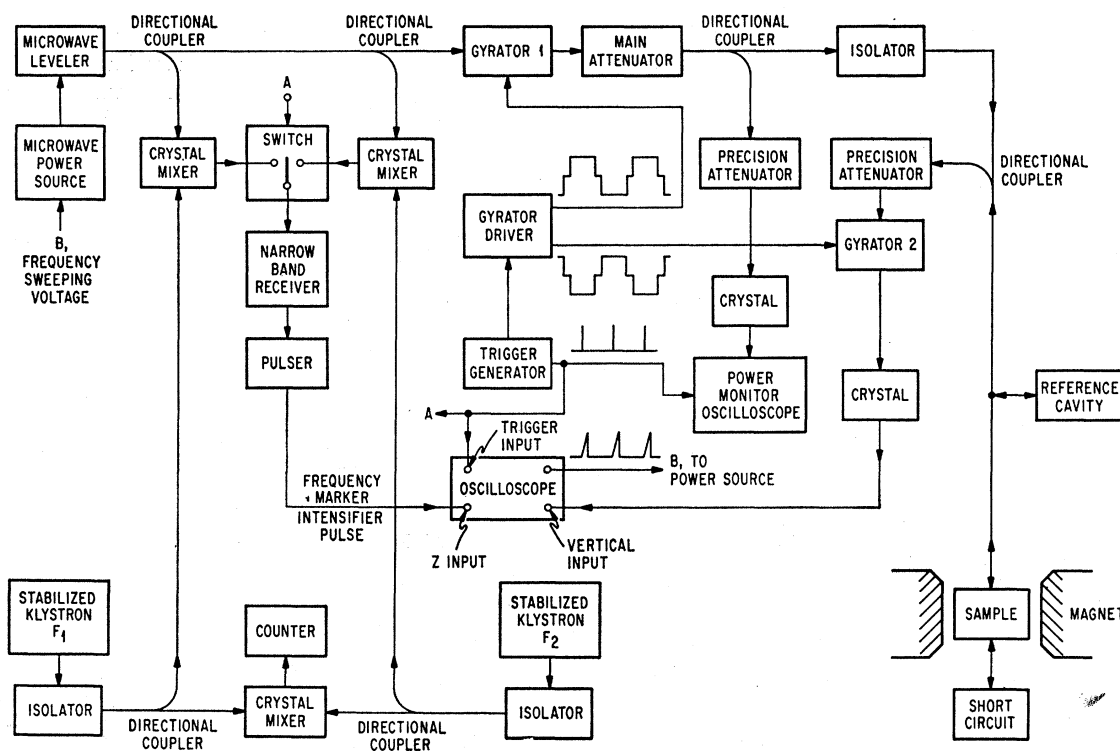


FIG. 1. Block diagram of experimental equipment.

the ambient temperature and by slow drifts in the equipment, in particular drifts of the dc magnetic field, were reduced by comparing the high- and low-power resonance frequencies in a short time interval. Shifts induced by sample heating from the absorption of microwave power were made negligible by sweeping the frequency through resonance very rapidly.

The essence of the procedure for measuring the frequency shift follows: Frequency markers were generated by mixing the outputs of frequency stabilized klystrons with the swept frequency signal, amplifying the beat signals with a narrow band amplifier, and using the resulting pulses to intensify the sweep. When the markers from the two klystrons were positioned at the peaks of the low- and high-power absorption signals on the oscilloscope screen, the beat frequency of the two klystrons, which was measured by an electronic counter, was the frequency shift.

A more complete description of the procedure follows: Figure 1 is a block diagram of the equipment. All measurements were performed at 9 Gc/sec and room temperature. The microwave power was generated by a traveling wave tube, amplified by a backward wave oscillator, and then passed through a power leveler. The frequency was swept through resonance 120 times/sec by the application of a sawtooth from the display oscilloscope to the traveling wave tube. Gyrator 1 in the main microwave line attenuated alternate sweeps and the ratio of the high to low power was adjusted by varying the current through this gyrotor. The power

incident upon the sample was sampled by a directional coupler terminated in a matched crystal detector, whose output was displayed on the power-monitor oscilloscope. The oscilloscope had been calibrated at a single low-power reference level by replacing the sample with a matched bolometer. The main attenuator adjusted the low-power signal to this reference level. The high-power level was determined by using the precision attenuator to find the attenuation necessary to reduce the high-power signal to the reference level. The power levels determined by this procedure do not depend upon the characteristics of the crystal detector. The reflected power was sampled by a second directional coupler which was also terminated by a matched detector. The signal was observed on the oscilloscope whose sweep was synchronized with the sawtooth signal which was applied to the traveling wave tube. In the absence of a sample resonance, the short circuit reflected power equal to the incident power. When the proper dc magnetic field was applied, a resonance absorption peak was observed in the reflected power as the frequency of the microwave power was swept through resonance. In order to provide a convenient display of the high- and low-power absorption, the amplitude of the high-power signal was reduced by pulsing gyrotor 2 out of phase with gyrotor 1. The high- and low-power signals observed on the oscilloscope screen could thus be set to equal amplitude. Errors introduced by the distortion of the absorption curves by the nonlinear crystal detector were negligible when the two signals were equal.

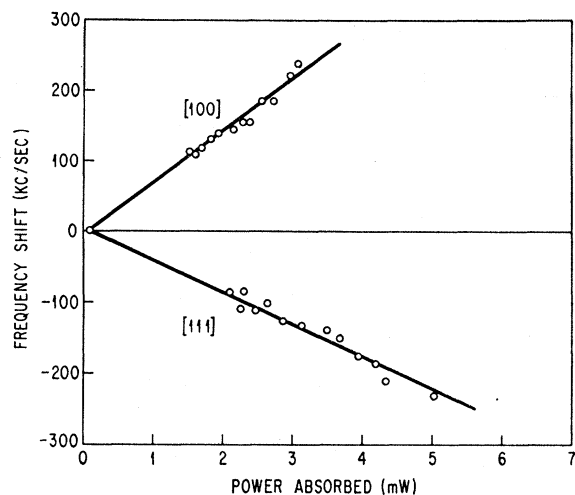


FIG. 2. Frequency shift as a function of power absorbed for a sample oriented with [100] and [111] crystallographic directions parallel to the dc magnetic field.

The actual frequency measurements were accomplished as follows: Microwave power from a klystron stabilized at frequency F_1 was mixed with a sample portion of the frequency-modulated microwave power, and the beat signals were amplified by a narrow band amplifier tuned at 5 Mc/sec. Whenever the swept klystron frequency was 5 Mc/sec above or below the frequency of the stabilized oscillator, the amplifier would pass a signal. The output of the amplifier was shaped by a pulse-forming network, and then applied to the z input of the signal oscilloscope. The pulses intensified the trace on the oscilloscope when the swept frequency was $F_1 \pm 5$ Mc/sec. Another set of frequency markers was generated with a second klystron tuned to F_2 . A switch at the input of the narrow band receiver synchronized the markers at $F_1 \pm 5$ Mc/sec with the low-power absorption signal and the markers at $F_2 \pm 5$ Mc/sec with the high-power signal. When the lower frequency markers were positioned at the peaks of the absorption signals, the difference in frequency of the klystrons was the frequency shift. The difference was determined by mixing the signal from the klystrons and measuring the beat frequency with an electronic counter. Final trimming of the circuit was accomplished with the aid of a reference cavity in the branch to the sample. The equipment was properly adjusted when the frequency of the absorption peak from the reference cavity was independent of the power level.

A typical set of data is shown in Fig. 2. The low-reference power level was 0.2 mW. The frequency was swept through the absorption curve in approximately 10 μ sec. Heating effects were already negligible at sweep speeds of the order of a millisecond. The estimated accuracy of a data point, which represents the average of ten readings, is 10 kc/sec.

The yttrium iron garnet single crystals used in this experiment were grown from a lead-oxide lead-fluoride

flux.¹⁸ The samples were prepared by tumbling them in a tunnel-like enclosure with abrasive loaded epoxy walls.¹⁹ The finest polish, which was with nominal one-half micron diamond, was followed by a one hour anneal at 900°C and slow cooled. The typical sample had a half-width of 0.3 Oe and a diameter of 0.6 mm.

Two different techniques for mounting the samples were used. One method was to orient the sphere by x-ray diffraction techniques and mount it on a quartz rod with the [110] axis parallel to the rod. In the other method, the sample was positioned within a Teflon pulley. The pulley could be rotated about two axes. The sample was then rotated until the magnetic field for resonance was either a maximum or minimum which corresponded to the hard or easy direction, respectively. Results by both methods were in agreement, but the second had a substantial advantage because of its speed.

IV. EXPERIMENTAL RESULTS—LOW POWER

Frequency shift measurements were previously made⁶ on four spherical samples with the static magnetic field along the [100] and the [111] directions. The power absorbed by the samples was of the order of 10 mW, and at this power level typical frequency shifts were of the order of 100 kc/sec. The shifts were found to be directly proportioned to rf power for all samples. Although the uncertainties associated with the measurements were larger than desired, the results of the analysis of these measurements indicated considerable agreement with

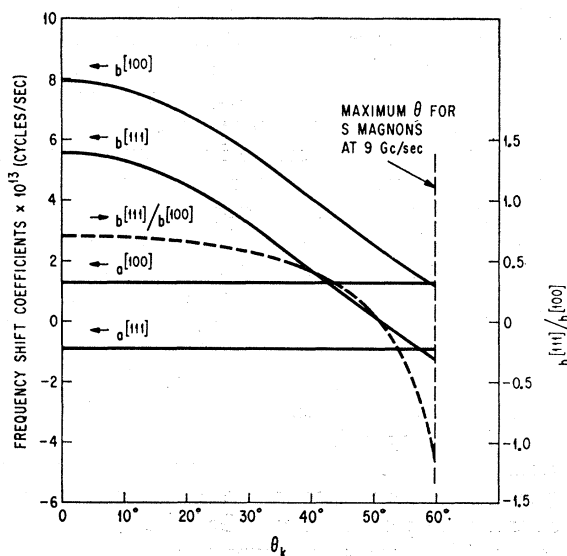


FIG. 3. Theoretical values of the frequency shift coefficients and the ratio $b^{[111]}/b^{[100]}$ for magnons degenerate with the $k=0$ magnon versus θ_k , the angle the magnon wave vector makes with the dc magnetic field. The frequency-shift coefficients are defined by the relation $\Delta f = a^{[i]}n_0 + \sum_{k \neq 0} b_k^{[i]}n_k$, where $[i]$ signifies crystallographic direction parallel to dc magnetic field. The arrow next to each coefficient points to the appropriate scale for that variable.

¹⁸ J. W. Nielsen, J. Appl. Phys. 31, 51S (1961).

¹⁹ H. S. Belson, Rev. Sci. Instr. (to be published).

the predictions of the pit-scattering theory of Sparks, Loudon, and Kittel.⁸ We have now improved the measuring technique and reduced the uncertainties in the results, and we have taken additional data. In particular, the surface of a sphere of yttrium iron garnet has been roughened, and the line width and the shift in the resonance frequency measured at a number of different surface roughnesses. A typical measurement of frequency shift as a function of power for both the [100] and [111] directions is shown in Fig. 2.

In order to obtain the coefficients $a^{[i]}$ and $b_k^{[i]}$ of Eqs. (30) and (31), M was measured as a function of temperature using a magnetization balance, and K_1/M was evaluated as a function of temperature from the measurements of the resonance frequency in the hard and easy directions. The value obtained for the anisotropy coefficient from our measurements is in good agreement with that obtained using Dillon's values⁶ for the anisotropy constant K_1 and published magnetization data²⁰ for YIG.

For two-magnon relaxation processes (such as surface-pit scattering), $k=0$ magnons scatter to $k \neq 0$ degenerate magnons (S magnons). These S magnons in turn relax to other magnons and the lattice. However, the S magnons dominate the n' population and we shall assume that only S magnons are excited. The values of b_k as calculated from Eq. (31) are plotted in Fig. 3 as a function of θ_k for S magnons, i.e., magnons such that $\omega_k = \omega_0$. This plot is appropriate for a resonance at 9 Gc/sec on yttrium iron garnet at room temperature. The a 's are also shown. Note that while $b_k^{[100]}$ is positive for all θ_k , $b_k^{[111]}$ is positive for $\theta_k < 51^\circ$, but negative for $\theta_k > 51^\circ$. This is quite important in the extraction of information from the observations.

Using the measured values of the frequency shift, the values of $a^{[i]}$ given in Eq. (30) and shown in Fig. 3, and the values of n_0 obtained from Eq. (37), we can easily

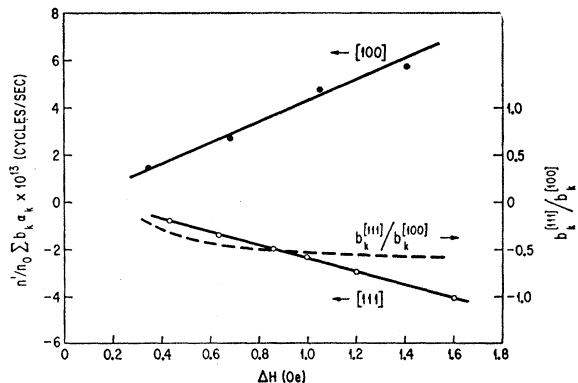


FIG. 4. Experimental value of $n'/n_0 \sum_{k \neq 0} b_k \alpha_k$ for the sample oriented with [100] and [111] axis parallel to the dc magnetic field and the ratio of these quantities, $b_k^{[111]}/b_k^{[100]}$, versus the half-width of the sample.

²⁰ J. Smit and H. P. J. Wijn in *Ferrites* (John Wiley & Sons, Inc., New York, 1959), p. 213.

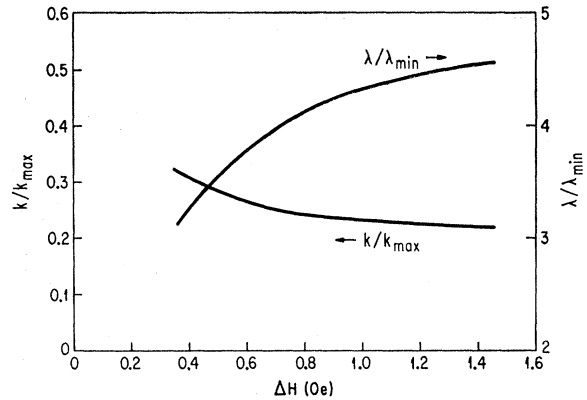


FIG. 5. Experimental values of k/k_{\max} and λ/λ_{\min} as a function of the half-width of the sample.

compute the difference $(\Delta f^{[i]}/n_0^{[i]}) - a^{[i]}$ which appears in Eq. (38). Thus, we are able to compute the quantity $n'/n_0 \sum_{k \neq 0} \alpha_k b_k$ for both the [100] and the [111] directions. These results plotted as a function of ΔH are shown in Fig. 4. This quantity is positive for the [100] direction and negative for the [111] direction for all the surface finishes. Since b_k for the [111] direction is negative only in the region $\theta_k > 51^\circ$, the predominant contribution to the sum must come from this region of k space. This conclusion does not require the assumption that only magnons degenerate with the $k=0$ magnon are excited since the form of b_k as a function of θ_k is only weakly dependent on the energy of the spin waves, as can be seen from Eq. (31). In fact, it can be concluded from our measurements that the magnon population is dominated by magnons in the region $50^\circ < \theta_k < 70^\circ$ for any physically possible energy distribution.

In order to analyze the data further, it is necessary to make assumptions concerning the relationship between n'/n_0 and α_k in the two directions. It is reasonable to assume that n'/n_0 as well as α_k are the same for a [100] and a [111] resonance for a given value of the half-widths in the two directions. If we assume that all of the S magnons which are excited by the pit scattering have the same \mathbf{k} , we can determine both the effective wave vector, \mathbf{k}_{eff} , and the ratio of n'/n_0 . Under these assumptions, the ratio of the quantities $n'/n_0 \sum_{k \neq 0} b_k \alpha_k$ for the two directions is just the ratio of the b_k 's of the effective wave vector for the two directions. This experimentally determine ratio $b_{k_{\text{eff}}}^{[111]}/b_{k_{\text{eff}}}^{[100]}$ is plotted as a function of ΔH in Fig. 4. The computed ratio $b_k^{[111]}/b_k^{[100]}$ as a function of θ_k is shown in Fig. 3. From these two curves one can obtain $\theta_{k_{\text{eff}}}$ and k_{eff} for each surface treatment. The effective wavelength λ_{eff} is just $\lambda_{\text{eff}} = 2\pi/k_{\text{eff}}$, and the ratio k_{eff}/k_{\max} and $\lambda_{\text{eff}}/\lambda_{\min}$ are plotted in Fig. 5 as a function of ΔH . The k_{\max} , the maximum wave vector that a S magnon can have, is given by the expression

$$k_{\max} = (4\pi M/3)^{1/2} (\gamma \hbar / D)^{1/2}, \quad (43)$$

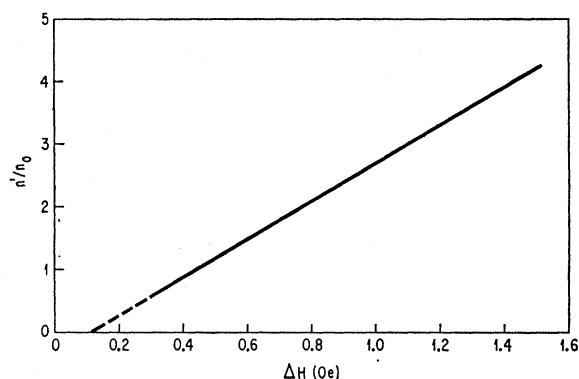


FIG. 6. Values of n'/n_0 as a function of the half-width of the sample deduced from experimental values of $b_k^{[111]}/b_k^{[100]}$. Dashed portion of curve is an extrapolation.

where D is the exchange constant. Therefore, for YIG,

$$k_{\max} = 3.4 \times 10^5 \text{ cm}^{-1} \quad (44)$$

and the corresponding minimum wavelength is

$$\lambda_{\min} = 1.8 \times 10^{-5} \text{ cm} \quad (45)$$

$$= 0.18 \mu. \quad (46)$$

The ratio of $\lambda_{\text{eff}}/\lambda_{\min}$ varies from 3.25 at $\Delta H = 0.4$ Oe to 4.55 at $\Delta H = 1.4$ Oe. Thus, λ_{eff} varies from 0.58μ at $\Delta H = 0.4$ Oe to 0.82μ at $\Delta H = 1.4$ Oe.

Sparks, Loudon, and Kittel⁸ have calculated the surface pit-scattering linewidth contribution and find good agreement with experimental results.²¹ As would be expected, the uniform mode relaxes most readily to those spin-wave states of wavelength $\lambda = 2\pi/k \approx R$, where the pit size R is approximately the same as the size of the polish grit. The initial measurements were made on a sample which had been polished with 0.5μ grit. The sample was then roughened by polishing with a larger grit for varying lengths of time. Thus, the linewidth presumably increased both because larger pits were produced and because a larger number of pits were present. The progressive increase in λ_{eff} is, therefore, in good qualitative agreement with the surface scattering theory.

Since $\theta_{k\text{eff}}$ has now been determined as a function of ΔH , it is a simple matter to obtain the corresponding $b_{k\text{eff}}^{[100]}$ and $b_{k\text{eff}}^{[111]}$ from Fig. 3. Using these values of $b_{k\text{eff}}^{[100]}$ and $b_{k\text{eff}}^{[111]}$ and Fig. 4, we are able to determine n'/n_0 as a function of ΔH as shown in Fig. 6. The linear relationship of n'/n_0 and ΔH is to be expected as we shall now show. Consider the kinetic equation for n_k , where k is the effective wave vector for the pit scattering. The rate at which such magnons are created is $\gamma\Delta H_{\text{ps}}n_0$ where ΔH_{ps} is the pit-scattering contribution to the resonance linewidth. The rate at which such magnons are destroyed is $\gamma\Delta H_k n_k$, or since $n_k = n'$, $\gamma\Delta H_k n'$, where ΔH_k is the linewidth associated with the

relaxation of the k th spin wave. Thus, the kinetic equation for n_k or n' is

$$\dot{n}' = \gamma\Delta H_{\text{ps}}n_0 - \gamma\Delta H_k n'. \quad (47)$$

In equilibrium

$$n'/n_0 = \Delta H_{\text{ps}}/\Delta H_k. \quad (48)$$

Thus, n'/n_0 is linearly proportional to ΔH_{ps} in agreement with the results shown in Fig. 6. That n'/n_0 is larger than 1 is no cause for concern since, in actuality, n' is distributed over many spin-wave states.

The curve in Fig. 6 extrapolates to $n'/n_0 = 0$ at a $\Delta H \approx 0.12$ Oe. This is presumably the "intrinsic" linewidth, i.e., nonsurface scattering, and agrees favorably with ΔH_k of long-wavelength spin waves as measured by parallel-pumping.²² Incidentally, the value of ΔH_k , the linewidth associated with the effective spin-wave state, can be determined from Eq. (48) and Fig. 6 and is found to be about 0.3 Oe, again agreeing in magnitude with the ΔH_k measured in the instability experiments.^{2,22}

As an additional consequence of their model, Sparks, Loudon, and Kittel⁸ propose that pit scattering brings about rapid equilibration of the S modes so that all these degenerate modes are populated equally. Sparks²³ has more recently made a similar suggestion with respect to the spin waves degenerate with the spin waves excited in a parallel-pumping experiment. However, this rapid equilibration is not evident either in the parallel-pump experiment²⁴ or in our frequency-shift experiment. Indeed we find that the distribution of magnons is dominated by magnons with $\theta_k > 51^\circ$.

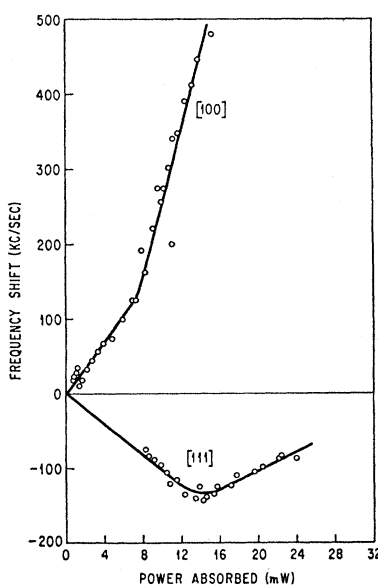


FIG. 7. Frequency shift as a function of power absorbed in the high-power region for a sample oriented with the [100] and [111] crystallographic directions parallel to dc magnetic field.

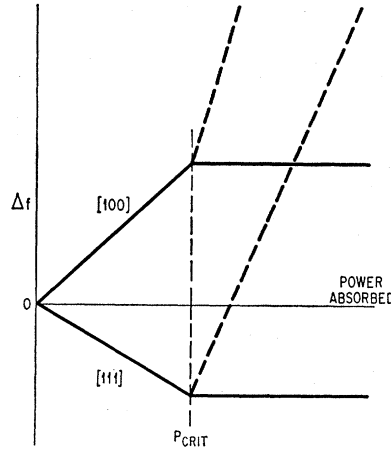
²² T. Kasuya and R. C. LeCraw, Phys. Rev. Letters 6, 223 (1961).

²³ M. Sparks, Phys. Rev. Letters 8, 54 (1962).

²⁴ T. Kohane and E. Schlömann, J. Appl. Phys. 34, 1544 (1963).

²¹ R. C. LeCraw, E. G. Spencer, and C. S. Porter, Phys. Rev. 110, 1311 (1958).

FIG. 8. Theoretical frequency shift versus power absorbed for a sample oriented with the [100] and [111] crystallographic directions parallel to the dc magnetic field. For powers larger than P_{crit} , the solid line indicates the contribution from n_0 and n' only, and the dashed line shows the total contribution from n_0 , n' and $n_{\theta_k=0}$.



V. EXPERIMENTAL RESULTS-HIGH POWER

In addition to measuring the shift in the resonance frequency at power levels below that necessary for the onset of instability (i.e., powers such that the susceptibility χ'' is independent of power), we have also observed the shift in resonance frequency at powers up to about twice that at which the onset of nonlinearity occurs in a number of YIG samples. We find that there is a fairly sharp change in the slope of the curve of the resonance frequency shift versus absorbed power; this change occurs roughly at the power at which χ'' begins to show a decline.

In general, the change in the slope of the curve of frequency shift versus power absorbed is most pronounced for well-polished samples; data for such a YIG sample is shown in Fig. 7. As the sample surface is roughened, the change in the slope diminishes. For very rough samples there is no measurable change in the slope of the curve, even though χ'' has decreased appreciably from its low-power values.

According to theory,¹ the spin waves which first become unstable are those which are degenerate with the uniform mode and which propagate parallel to the applied field ($\theta_k=0$, $k=k_{\text{max}}$). These spin waves build up to amplitudes comparable to that of the homogeneous mode. The amplitude of the homogeneous mode is "clamped" at its magnitude at the threshold for instability, for any increase in amplitude would drive additional spin waves unstable thereby providing parallel routes for transfer of energy to the lattice. Thus, the number of magnons of each type, above the threshold power, is

$$n_0 = \frac{P_{\text{abs, crit}}}{\gamma \hbar V \omega_0 \Delta H} \quad (\text{"clamped"}), \quad (49)$$

$$n' = \frac{\Delta H_{\text{ps}} P_{\text{abs, crit}}}{\Delta H_k \gamma \hbar V \omega_0 \Delta H} \quad (\text{"clamped," being proportional to } n_0), \quad (50)$$

and

$$n_{\theta_k=0} = \Delta P / \gamma \hbar V \omega_0 \Delta H_k, \quad (51)$$

where ΔP is the power absorbed in excess of the critical power and ΔH_k is the linewidth associated with the $\theta_k=0$ magnons. Equations (49) and (50) are obtained from Eqs. (37) and (48). Equation (51) is analogous to Eq. (37) for n_0 . Since

$$P_{\text{abs, crit}}/V = \Delta H \Delta H_k \omega_0 / 8\pi, \quad (52)$$

Eq. (51) can be rewritten in the form

$$n_{\theta_k=0} = \frac{\Delta P}{P_{\text{abs, crit}}} \frac{\Delta H}{8\pi\gamma\hbar}. \quad (53)$$

The resultant frequency shift, above the threshold, is given by

$$\Delta f^{[i]} = a^{[i]} n_0^{[i]} + b_{\theta_{k_{\text{eff}}}}^{[i]} n'^{[i]} + b_{\theta_k=0}^{[i]} n_{\theta_k=0}^{[i]}, \quad (54)$$

where the $b_{\theta_k=0}^{[i]}$ are given by Eq. (31) with $\theta_k=0$ or obtained from Fig. 3 and n_0 , n' , and $n_{\theta_k=0}$ are given by Eqs. (49), (50), and (53). Since ΔP , $P_{\text{abs, crit}}$, and ΔH can be measured and $b_{\theta_k=0}^{[i]}$ calculated, the magnitude of the $\theta_k=0$ contribution to the shift can be predicted. The $b_{\theta_k=0}^{[i]}$ are both positive and several times larger in magnitude than those corresponding to the $\theta_{k_{\text{eff}}}$ of pit scattering, and the $\theta_k=0$ shifts should be large and positive in both directions. The frequency shift as a function of power absorbed for the idealized case is shown in Fig. 8, the solid lines indicating the contribution of n_0 and n' and the dotted lines showing the total contribution of n_0 , n' and $n_{\theta_k=0}$ above the critical power.

The slope of the high-power portion of the curve in Fig. 8 is from Eqs. (53) and (54)

$$b_{\theta_k=0}^{[i]} = \frac{1}{P_{\text{abs, crit}}} \frac{\Delta H}{8\pi\gamma\hbar}. \quad (55)$$

All of the slopes measured were smaller in magnitude than those calculated from Eq. (55). One possible explanation for this behavior is that some spin wave other than the $\theta_k=0$ spin wave is responsible for the instability. Since $b_{\theta_k=0}^{[i]}$ is the maximum value of $b_k^{[i]}$ in both the [100] and [111] directions (see Fig. 3), the $b_k^{[i]}$ of any other spin wave would necessarily be smaller and result in a smaller slope. Inversely, the observed slope determines a particular value of θ_k , and we find that the value so determined from observations taken in the [111] direction then predicts a slope in the [100] direction which is in satisfactory agreement with observations. As an example, consider the data shown in Fig. 7. The low-power region can be fit by a $\theta_{k_{\text{eff}}}$ of about 55° and a $k_{\text{eff}} \approx 0.3k_{\text{max}}$. The high-power region gives for the unstable spin wave an experimental value for θ_k of about 45° and a $k \approx 0.55k_{\text{max}}$. The experimental value of the k of the unstable mode is always found to be between k_{eff} and k_{max} .

The discrepancy between predictions based on the usual instability theory and experiment may arise because of the presence of pit scattering. The two-magnon

pit-scattering terms in the Hamiltonian are second order in the creation and destruction operators and can, in principle, be diagonalized yielding new normal modes or spin waves. The new modes will be linear combinations of the old modes; the greater the strength of the pit-scattering terms, the greater the amount of admixing of the old modes. The fourth-order dipolar terms in the Hamiltonian, which are the source of the instability, would then have to be expressed in terms of these new normal modes. The new mode which would become unstable, being a linear combination of old modes, would necessarily shift the resonance frequency less than the $\theta_k=0$ spin waves since the new "averaged" b would be less than $b_{\theta_k=0}$. However, it is not clear why this "averaged" b approaches $b_{\theta_{k,eff}}$ as the sample is roughened.

Finally, we caution that the apparent disparity between the observed slope in the high-power region and that predicted by Eq. (55) may be a result of the limited range of power over which data could be taken. Schlömann^{2,10} and Suhl²⁵ have considered explicitly the onset of instability in the presence of a two-magnon relaxation process (in our case, surface pit scattering) and have shown that the characteristics of the onset of instability depend in a very pronounced manner upon the ratio of the "intrinsic linewidth" (from other than two-magnon scattering) to the linewidth from two magnon scattering. When there is no two-magnon scattering, there is a sharp discontinuity in the slope of the χ'' versus power curve; this discontinuity occurs at the critical power. As the amount of two-magnon scattering increases the discontinuity in the slope of the χ'' versus power curve vanishes; the decrease in χ'' begins

at power levels which are well below the critical level and the χ'' curve falls off gradually with increasing power.²⁶ This gradual onset of instability (which we observe in our χ'' curves) presumably arises because of the relatively large number of spin waves excited through pit scattering. The critical power is no longer sharply defined, except as a parameter characteristic of the asymptotic behavior of χ'' at high-power levels. The critical amplitude of the mode of uniform precession is never actually attained, but is only approached asymptotically.¹⁰ A similar behavior would be expected in the frequency shift curve; the transition from the low-power to the high-power slope should be gradual, and the high-power slope is asymptotically approached. We took data at powers up to about twice that at which a change in the slope of the frequency shift curve (and χ'' curve) occurs. It is possible that the high-power slope asymptote is not reached over this range of power. Unfortunately, it is impossible to observe the frequency shift at still higher power levels since the resonance here becomes so wide and so distorted that it is impossible to identify the resonance frequency precisely and thereby measure a resonance frequency shift.

ACKNOWLEDGMENTS

The authors wish to express their appreciation to H. Callen for many valuable discussions, to W. Luciw for his ingenious and informed experimental aid, to J. Douglas for technical assistance, and to J. Clark and G. R. Harrison of the Sperry Microwave Electronics Division at Clearwater, Florida, for supplying us with some of the YIG samples.

²⁵ H. Suhl, *J. Appl. Phys.* **30**, 1961 (1959).

²⁶ For experimental verification, see, M. T. Weiss, *J. Appl. Phys.* **31**, 778 (1960).